Natural Hazards (2019) 96:389–412
https://doi.org/10.1007/s11069-018-3548-9

ORIGINAL PAPER

Assessment of co-seismic landslide hazard using the Newmark model and statistical analyses: a case study of the 2013 Lushan, China, Mw6.6 earthquake

Siyuan Ma[1] · **Chong Xu**[1]

Received: 2 February 2018 / Accepted: 28 November 2018 / Published online: 5 December 2018

Abstract
The April 20, 2013 Mw6.6 earthquake of Lushan County, Sichuan Province, China, has triggered 4540 landslides (> 1000 m^2). Exploring a more effective method to assess landslide hazard in the affected area of this event is of great significance for disaster prevention and mitigation. By applying the Newmark model and two statistical analysis models (logic regression and support vector machine, LR and SVM), this study addressed this issue. In the Newmark model, we used the landslide point density, the average gradient (mean slope) and the mean peak ground acceleration to group the lithology and created a critical acceleration (a_c) map. The Newmark displacements and the probability of the slope instability are mapped by combining the a_c map and PGA map. In the statistical analysis models of LR and SVM, 7040 samples (4540 landslide sites and 2500 random non-landslide sites) were randomly divided into the training set (5000 samples) and validation set (2040 samples). Based on the relationship between landslide distribution and influence factors, we selected the critical acceleration (a_c) value, topographic relief, PGA, and distance to rivers as the independent variables for LR and SVM. Finally, the ROC curves for three landslide hazard models were drawn and the AUC values were calculated. The landslide hazard maps produced by LR are similar to those by applying SVM. The AUC values indicate that these two models combined with a_c data perform better than the simplified Newmark model. In this study, a new method of integrating statistical analysis models (LR and SVM) with critical acceleration (a_c) for earthquake landslide hazard assessment is presented, which can be used to carry out seismic landslide hazard assessment more effectively than the simplified Newmark model.

Keywords Lushan earthquake · Co-seismic landslides · Hazard · Newmark model · Statistical analysis

✉ Chong Xu
xuchong@ies.ac.cn; xc11111111@126.com

[1] Key Laboratory of Active Tectonics and Volcano, Institute of Geology, China Earthquake Administration, Beijing 100029, China

1 Introduction

Co-seismic landslides can cause significant economic losses and casualties and thus have received much attention of researchers in the community of geosciences in recent years (Keefer 1984; Rao et al. 2017; Xu et al. 2014, 2016, 2018). Many studies focus on landslide inventory, slope-failure statistics and hazard assessment, providing important support for mitigation of earthquake-induced landslide hazard (Nowicki et al. 2014; Xu and Xu 2012; Xu et al. 2012a, 2015, 2016). Currently, the commonly used methods of landslide hazard assessment include statistical analysis methods and Newmark model method. The statistical analysis (Akgun 2012; Kavzoglu et al. 2015; Nowicki Jessee et al. 2018; Nowicki et al. 2014; Ohlmacher and Davis 2003; Xu et al. 2012b, 2013a) uses co-seismic landslide inventories to establish the mathematical statistical models between these landslides and landslide-related factors, including hydrology, geology, topography and human activity. According to the established models, the landslide hazard assessment of the whole study area is conducted. At present, there has been massive assessment based on mathematical statistical analysis, especially those based on the logic regression (LR) (Bai et al. 2015; Huang et al. 2015; Lee 2005; Umar et al. 2014; Xu et al. 2013b) and support vector machine (SVM) (Hong et al. 2015; Kavzoglu et al. 2015). These two statistical analysis methods have been widely used for the regional landslide hazard prediction and achieved good results. The advantages of these statistical methods are that the establishments of models are based on real landslide distribution, and the assessment results are relatively objective. But they lack the understanding of landslide occurrence mechanism.

The Newmark (1965) method estimates co-seismic landslide displacement by modeling a landslide as a sliding block on an inclined plane that has a known critical or yield acceleration. (The ground acceleration needed to overcome sliding resistance and initiate downslope movement.) The modeled displacement is used as an index to judge the seismic stability of the slope. (Al-Homoud and Tahtamoni 2000; Dreyfus 2011; Dreyfus et al. 2013; Godt et al. 2008; Jibson et al. 1998, 2000; Jibson and Michael 2009; Kaynia et al. 2011; McCrink 2001; Miles and Ho 1999). It is now widely used in assessment of geotechnical effects of co-seismic landslides in the world, such as the 1979 Coyote Lake earthquake (Wilson and Keefer 1983), 1994 Mw6.7 Northridge earthquake (Jibson et al. 2000), 1989 Mw6.9 Loma Prieta earthquake (McCrink 2001) and 2008 Mw7.9 Wenchuan earthquake (Godt et al. 2008). However, the Newmark model does not consider the related influencing factors aforementioned. Many studies have shown that these factors have important influences on the occurrence of landslides. Meanwhile, the prediction based on the Newmark model needs definite physical properties of rocks and ground motion parameter to calculate slope displacements (Pradel et al. 2005), while such data are usually difficult to acquire under the current technical conditions. So the landslide hazard assessment solely based on the Newmark model remains challenging.

Based on the distribution of landslides, this work used the Newmark model and two statistical analysis methods (LR and SVM) integrating with the output results of the Newmark method to conduct the landslide hazard assessment of the Lushan earthquake and hoped to find a more effective method for landslide hazard assessment. It would shed light on improving the seismic landslide prediction and a reference for disaster prevention and reduction in seismic areas.

2 Lushan earthquake and geological setting

The collision of the Indian and Eurasian plates resulted in the uplift of the Tibetan Plateau and eastward motion of a series of blocks in this highland. Obstructed by the rigid Sichuan Basin, the Longmenshan thrust zone formed along the boundary between the Tibetan Plateau and Sichuan Basin, at which the accumulated strain is released during frequent earthquakes. The April 20, 2013 Mw6.6 earthquake in Lushan, Sichuan, China, is another major shock following the 2008 Wenchuan Mw7.9 event on this fault zone (Fig. 1). It is composed of three thrust fault systems, which are the Maoxian–Wenchuan (also called Houshan), the Yingxiu–Beichuan fault (also called Zhongyang), and the Guanxian–Jiangyou fault (also called Qianshan) from northwest to southeast (Xu et al. 2009). These faults comprise a series of cascaded fractures of smaller scales. The 2013 Lushan earthquake occurred in the southwest section of the Longmenshan thrust zone. Its epicenter is located at the Shuangshi Dachuan fault (southwest section of Qianshan fault). No co-seismic surface rupture of this event was observed. Field investigations, focal mechanism solutions and spatial distribution of aftershocks indicated that the seismogenic fault of the Lushan quake is likely a blind reverse fault southeast of the Shuangshi–Dachuan fault (Xu et al. 2013c).

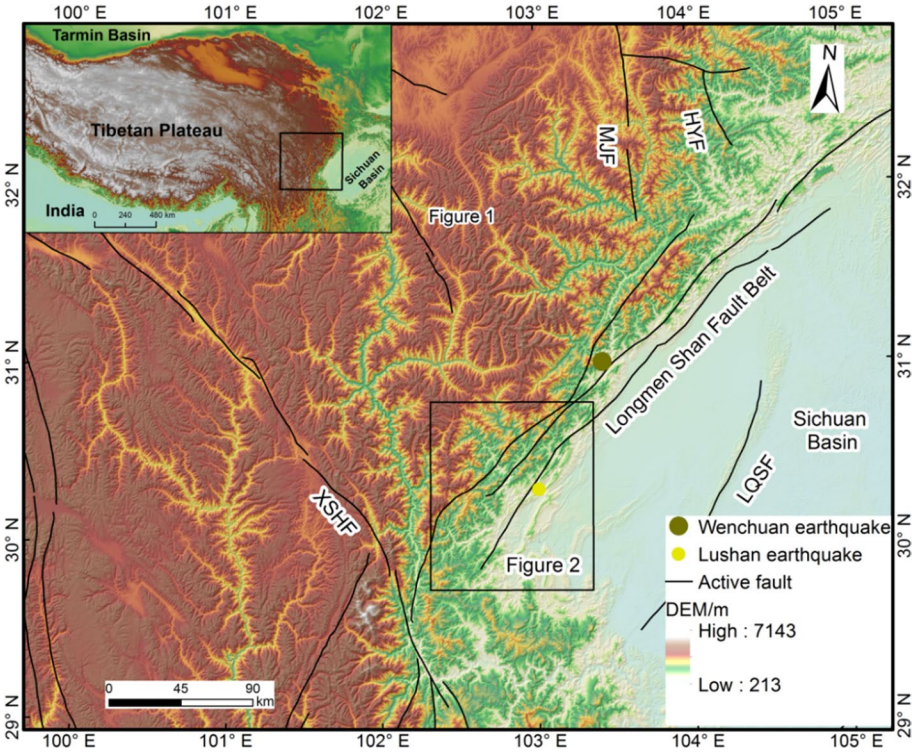

Fig. 1 Map showing topography and tectonics of the Tibetan Plateau's eastern margin. *MJF* Mingjiang fault, *XSHF* Xianshuihe fault, *HYF* Huya fault, *LQSF* Longquanshan fault. The active fault lines are from Deng et al. (2007)

3 Data and method

3.1 Methodology

3.1.1 Newmark displacement model

The Newmark displacement method was proposed for the stability of dams under earthquakes (Newmark 1965). It thinks the dam instability depends critically on the deformation of the dam, rather than the minimum safety factor. It simulates a landslide as a rigid friction block that slides on an inclined plane at a known critical (or yield) acceleration, a_c, which is simply the threshold base acceleration required to overcome shear resistance and initiate sliding. The analysis calculates the cumulative permanent displacement of the block relative to its base as it is subjected to the effects of an earthquake acceleration-time history. Those portions of the record that exceed the critical acceleration are integrated twice to obtain the cumulative displacement of the block (Jibson 1993).

The Newmark simplified model calculates three parameters: the safety factor (F_s), critical acceleration (a_c) and the cumulative displacement (D_n).

According to the geometric properties [soil thickness (t), the degree of soil saturation (m); slope angle (α)] and mechanical properties [effective cohesion (c'), internal friction angle (ψ'), unit weight of soil and rock (γ) and unit weight of underground water (γ_w)], we can calculate the safety factor (F_s) by Eq. (1):

$$F_s = \frac{c'}{\gamma t \sin\alpha} + \frac{\tan\psi'}{\tan\alpha} - \frac{m\gamma_w \tan\psi'}{\gamma \tan\alpha} \tag{1}$$

The critical acceleration (a_c) is calculated by the safety coefficient F_s based on the infinite slope method (Eq. 2):

$$a_c = \left(F_s - 1\right) g \sin\alpha \tag{2}$$

Simplified regression models to estimate Newmark displacement are regressed by analysis of strong ground motion records. At present, many researchers have fitted different Newmark models based on the global strong-motion records (Bray and Travasarou 2007; Jibson 2007; Jibson et al. 1998; Rathje 2008; Saygili and Rathje 2008). According to the 2270 strong-motion records of 30 worldwide earthquakes, Jibson (2007) obtained different simplified Newmark models based on different ground motion parameters. In this study, we selected one of the Newmark models using PGA. The Newmark displacement maps were prepared by combining the a_c map and PGA map based on Eq. (3)

$$\log D_n = 0.215 + \log\left[\left(1 - \frac{a_c}{\mathrm{PGA}}\right)^{2.341} \times \left(\frac{a_c}{\mathrm{PGA}}\right)^{-1.438}\right] \tag{3}$$

where D_n is the Newmark displacement, a_c is the critical acceleration, and PGA is the peak ground acceleration.

3.1.2 Logistic regression (LR)

The logistic regression approach has widely been used for landslide hazard assessment in recent years and become the most common methodology in the disaster assessment (Ayalew and Yamagishi 2005; Dai et al. 2001; Guzzetti et al. 1999; Nowicki Jessee et al. 2018; Nowicki et al. 2014; Umar et al. 2014). This algorithm applies maximum likelihood estimation after

transforming the dependent variables into the logic variables (the natural log of the odds of the dependent occurring or not) (Bai et al. 2015). In this way, the results of the logistic regression generate a useful formula for predicting the probability of presence or absence of a characteristic or outcome based on the values of a set of predictors. An equation predicting the landslide occurrence can be derived as follows, based on the description provided by Hosmer and Lemeshow (2005).

Quantitatively, the relationship between the probability of landslide occurrence and its dependency on several variables can be expressed as:

$$p = \frac{1}{(1 + e^{-z})} \tag{4}$$

where p refers to the estimated probability of landslide occurrence. The value of p is constrained within a range between 0 and 1, where 0 indicates a 0% probability of a landslide and 1 indicates a 100% probability. The term z is the linear combination of independent variables:

$$z = \beta_0 + \beta_1 \chi_1 + \cdots \beta_i \chi_i \tag{5}$$

where β_0 is the intercept of the model, i is the number of independent variables, β_i ($i = 1, 2, 3, \ldots, n$) is the slope coefficient of the model, and x_i ($i = 1, 2, 3, \ldots, n$) is the independent variable.

3.1.3 Support vector machine (SVM)

Due to the high nonlinearity of geological hazards, there are obvious shortcomings in the traditional statistical analysis method in expressing this nonlinearity. Researchers (Hu et al. 2007; Marjanović et al. 2011; San 2014; Yao et al. 2008) attempted to apply the support vector machine (SVM) for geological hazards evaluation and found that it is very suitable for spatial prediction of landslide hazard. It can solve the classified and fitting problems, which is characterized by distinctive superiority in solving the nonlinear problem and high-dimensional pattern recognition with less samples. It has stronger theoretical basis and better performance compared to the neural network learning algorithm.

Consider a set of linear separable training vectors x_i ($i = 1, 2, \ldots, n$). The training vectors consist of two classes, which are denoted as $y_i = \pm 1$. The goal of the SVM is to search for an n-dimensional hyperplane differentiating the two classes by the maximum gap. Mathematically, we minimize

$$\min \frac{1}{2} w^2 \tag{6}$$

subject to the following constraints

$$y_i \left(w \cdot x_i + b \right) \geq 1 \tag{7}$$

where $\|w\|$ is the norm of the normal of the hyperplane, b is a scalar base, and $\cdot$ denotes the scalar product operation. Introducing the Lagrangian multiplier, the cost function can be defined as

$$L = \frac{1}{2} w^2 - \sum_{i=1}^{n} \lambda_i \left(y_i \left(\left(w \cdot x_i \right) + b \right) - 1 \right) \tag{8}$$

where k_i is the Lagrangian multiplier. The solution can be achieved by dual minimizing Eq. (3) with respect to w and b through standard procedures, and the detailed discussions can be found in the literature (Marjanović et al. 2011).

For a non-separable case, one can modify the constraints by introducing slack variables:

$$y_i\left(w \cdot x_i + b\right) \geq 1 - \xi_i \tag{9}$$

Equation (8) can be modified as

$$L = \frac{1}{2}w^2 - \frac{1}{vn}\sum_{i=1}^{n}\xi_i \tag{10}$$

where v (0, 1] is introduced to account for misclassification. In the present study, + 1 and − 1 represent the failed and stable cases, respectively. One can easily see that stable cases are not available and have to be generated.

This study was based on the radial base kernel function (RBF) in version LIBSVM-3.22 (Chang and Lin 2011) and used the cross-validation method to optimize the parameters of the penalty factor C and the kernel function parameter.

3.2 Data sources and processing

The Lushan earthquake induced massive different types of landslides, including highly disrupted shallow slides and rock falls, deep landslides and large rock avalanches (Xu et al. 2015). According to the distribution of these landslides, the study area was defined as an elliptical area (Fig. 2), which covers 5396 km^2 with elevations 300 m to 6000 m. In lithology, the study area is dominated by sandstone, limestone, dolomite, mudstone, granite and quaternary sediments. The major rivers in the study area are the Xingjing River, Shiyang River, and Linguan River. Most seismic landslides are present along the two sides of these rivers (Fig. 2).

A detailed, accurate, objective, and complete co-seismic landslide database was employed in this study, which was derived from post-earthquake high-resolution aerial photographs and satellite images, as well as a series of pre-earthquake high-resolution satellite images. The previous work (Xu et al. 2015) indicated that the Lushan earthquake triggered 15,546 landslides larger than 100 m^2, of which 4540 pieces are larger than 1000 m^2 (Fig. 2). Considering the accuracy of data, these 4540 landslides were employed as the samples for this work. For the selection of non-landslide samples, we randomly chose 2500 samples in the landslide-free area, i.e., outside the buffer zone of landslide samples (buffer radius = 100 m). Finally, we got 7040 samples, from which we randomly selected 5000 samples for modeling (training), and the remaining 2040 samples were used for tests.

The resolution of DEM in the study area is 10 m. The topographic relief and slope angle were derived from this DEM. The river networks were also extracted from this DEM. Lithology was from the 1: 200,000 geological map.

At present, objective lithology classification and assignment based on geological maps remains one of the difficult problems for regional evaluation in the Newmark method (Gallen et al. 2015, 2016; Jibson et al. 2000). As different geological settings can lead to varied mechanical properties of rocks and soils, thus there may be a strong subjectivity in grouping the lithology based on the types of rock and soil masses. Gallen et al. (2015) used the Newmark model and co-seismic landslide inventory of the 2008 Wenchuan earthquake to invert material properties, and the results show that the strength inversion of rock

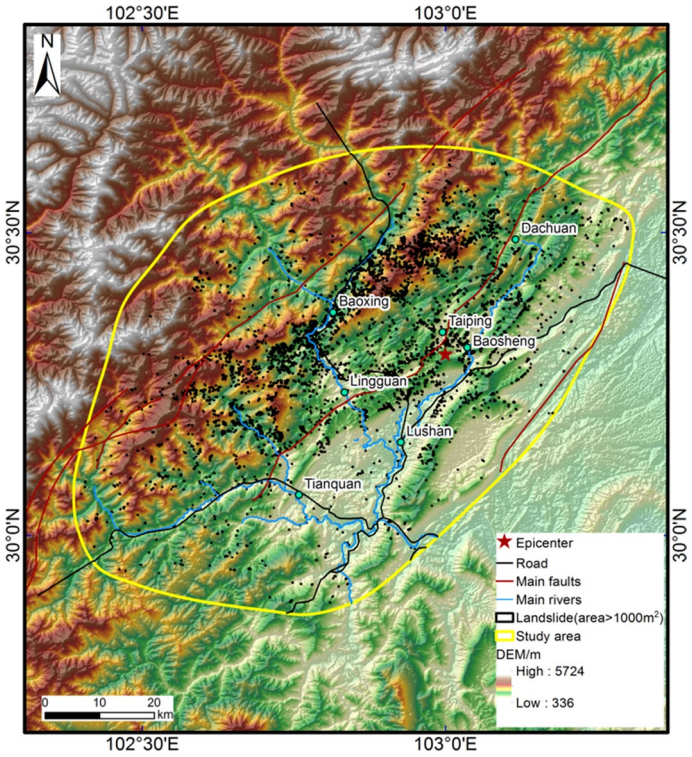

Fig. 2 The study area (yellow line) and Lushan earthquake-triggered landslides with area ≥ 1000 m^2

mass based on co-seismic landslide inventory is an effective method to improve the assignment of material properties. In addition, Jibson et al. (2000) argued that compared with the accurate mechanical parameters of lithology, the mechanical differences between different lithology groups may be more important for the prediction results of the Newmark model. So, in this study, we referred to the results of previous study (Xu et al. 2015), and obtained landslide density (LND), average slope gradient (mean slope) and average peak ground acceleration (mean-PGA) in homogeneous lithology ages by statistics. Meanwhile, according to the rock engineering standards used in China (Ministry of Water Resources of the People's Republic of China 2014), the rocks in the study area were classified into five types: hard (Group 1), relatively hard (Group 2), soft (Group 3), weak (Group 4) and loose (Group 5).

The lithology of hard type includes granite, diorite and intrusive rocks. However, due to the influence of geological structures, their actual strength should be obviously lower than that expected. As shown in Fig. 3, the landslide density in this group of rocks reached the maximum, 2/km^2. Therefore, appropriate reduction for mechanical values of Group 1 is made (the reduction coefficient is set to 0.7). The relatively hard type of rocks (Group 2) involves five strata: Pre-Sinian, Ordovician, Silurian, Devonian and Jurassic. The lithology is mainly composed of clasolites and carbonatites. Although the mean slope of this group is high, the values of both mean-PGA and the landslide density are small (Fig. 3). So it is reasonable that this rock mass is classified into the relatively hard rock.

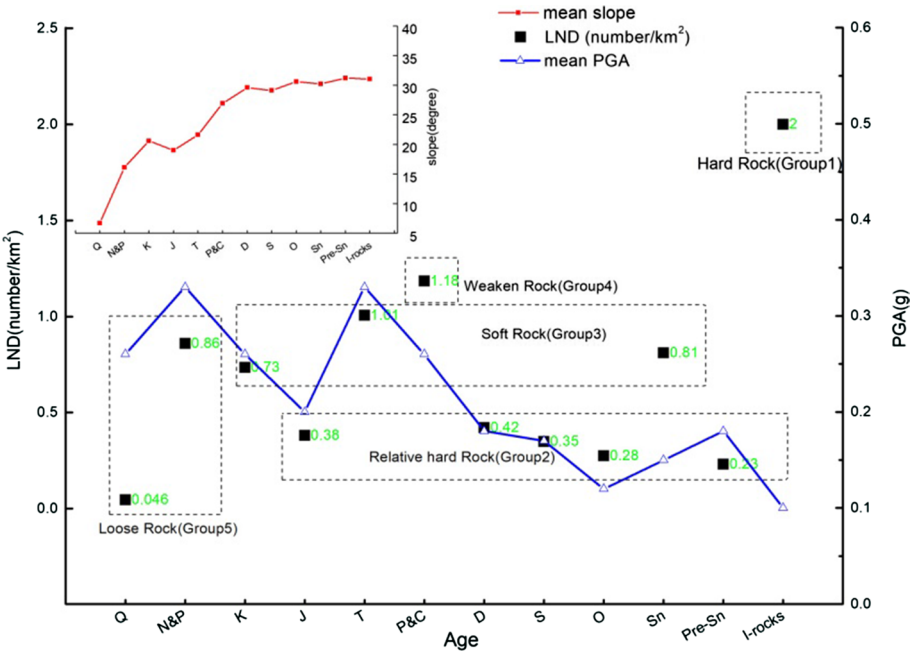

Fig. 3 Landslide density, mean value of slope and PGA in various lithology ages. *LND* landslide number density, *Q* quaternary, *N&P* neogene and paleogene, *K* cretaceous, *J* jurassic, *T* triassic, *P&C* permian and carboniferous, *D* devonian, *S* silurian, *O* ordovician, *Sn* Sinian, *Pre-Sn* Pre-Sinian, *I* intrusive rock

The strata of soft rock type (Group 3) involve three strata: Cretaceous, Sinian and Triassic. The lithology is mainly composed of sandstones, mudstones, dolomites and limestones. The values of landslides density in this rock type range from 0.73 to 1.01/km^2; of which that of Triassic strata reaches the maximum, 1.01/km^2. The reason for this phenomenon is due to the larger value of the PGA in the Triassic strata, which resulted in the higher landslide density than the other two strata.

The strata of weaken rock (Group 4) include Carboniferous and Permian. The lithology is dominated by limestones and siltstones, where the landslide density reached 1.18/km^2, and the value of PGA is not high with 0.26 g, so these two strata were considered as the weak rock type.

The Tertiary–Quaternary strata (Group 5) are of loose materials (alluvium and gravel, coarse conglomerate, siltstone). In Fig. 3, little landslides are present in the quaternary system. This is because the slope angle of this stratum is relatively low (generally less than 10°), so experienced small gravitational effect during the quake.

Conducting a Newmark analysis requires input data such as strong ground motion, shear strength, and slope angle. First of all, the depth of the failure surface was set to 3.0 m based on field observations and previous research (Dreyfus et al. 2013; Jibson et al. 2000). The pore water pressure ($m=0$ in Eq. 1) was neglected because of the dry condition during the temblor in the study area.

The strength parameters and details for each group are adopted from geotechnical bibliography (Ministry of Construction of the People's Republic of China 2009; Ministry of Water Resources of the People's Republic of China 2014) and previous studies

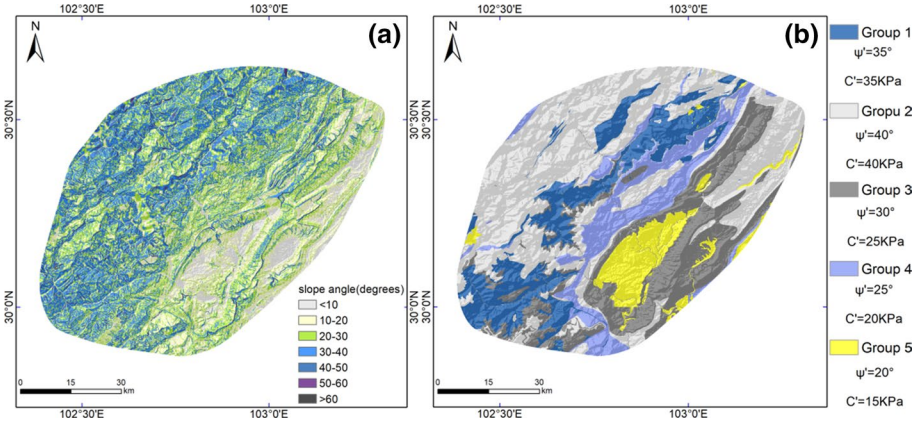

Fig. 4 Map showing distribution of slope angles and rock formations. **a** Slope angle; **b** strength groups

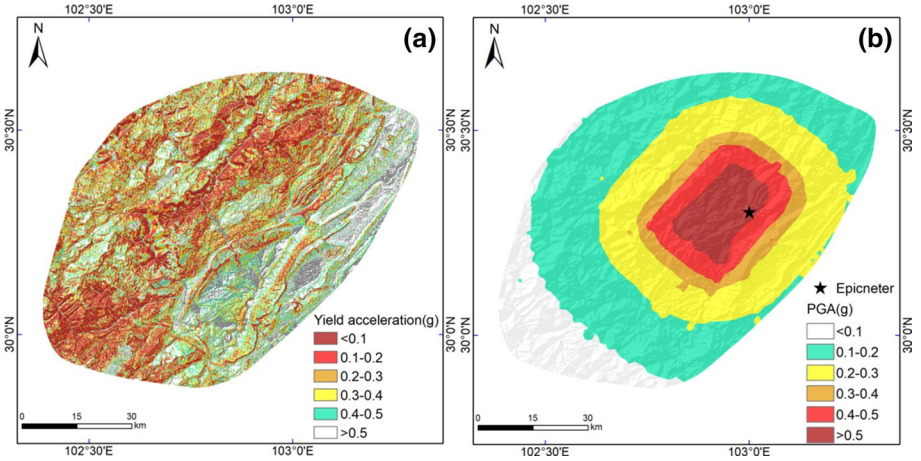

Fig. 5 Map showing distribution of critical acceleration (a_c) and PGA; **a** critical acceleration (a_c), **b** peak ground acceleration (PGA)

(Chen et al. 2014a; Dreyfus et al. 2013). The slope angles were derived from the DEM (10 m). The distribution of slope gradient (Fig. 4a) indicates that most of the study area hosts slopes with angles from 20° to 40°. Figure 4b shows the rock grouping and mechanical parameters of each group.

Using the input data, the factor-of-safety map (Fig. 5a) and the critical acceleration (a_c) map (Fig. 5b) were prepared using Eqs. 1 and 2, in which the a_c value represents a measure of intrinsic slope properties and can be identified as the seismic landslide susceptibility. Then, the Newmark displacement (Fig. 6) was estimated through the simplified Newmark model (Jibson 2007).

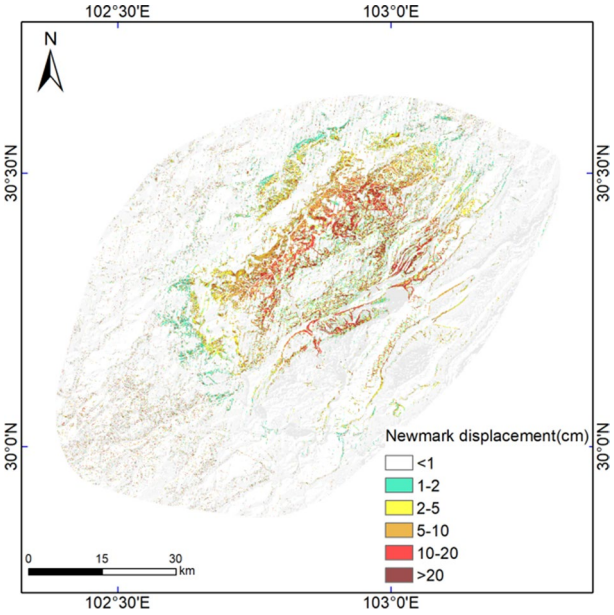

Fig. 6 Map showing distribution of Newmark displacements of the Lushan earthquake

3.3 Research process

The detailed flow chart of this study is shown in Fig. 7. The basic spatial database comprises the co-seismic landslide inventory, geological and topographic data, seismic data such as PGA, as well as other data derived from the above data. The research was divided into two parts: (1) the Newmark simplified model; (2) two statistical analysis models integrating with the Newmark model. In the Newmark model, we used the landslide number density (LND), the average slope gradient (mean slope) and the mean ground motion peak acceleration (mean-PGA) to group the lithology. A critical acceleration (a_c) map was prepared by combining with lithologic grouping results of the study area. The Newmark displacement map was compiled by combining the a_c map and PGA map of the study area, and the slope instability probability distribution was obtained based on the slope failure probability function.

In the two statistical analysis models (LR and SVM) integrating with the output results of the Newmark model, correlations between co-seismic landslide number density (LND) and six factors were analyzed. Four factors, critical acceleration (a_c), topographic relief, PGA and distance to rivers, were selected as the influencing factors of the Lushan earthquake landslides. Using the training samples, the landslide hazard assessment was carried out by the logistic regression model (LR) and support vector machine (SVM), respectively. Finally, the training set and test set were used to compare the landslide hazard evaluation results of three models.

4 Analysis of factors

At present, there is no widely accepted standard for the selection of influencing factors for landslide hazard assessment (Yalcin 2008), though selecting appropriate evaluation parameters is very important for establishing assessment models. In general, the occurrence of

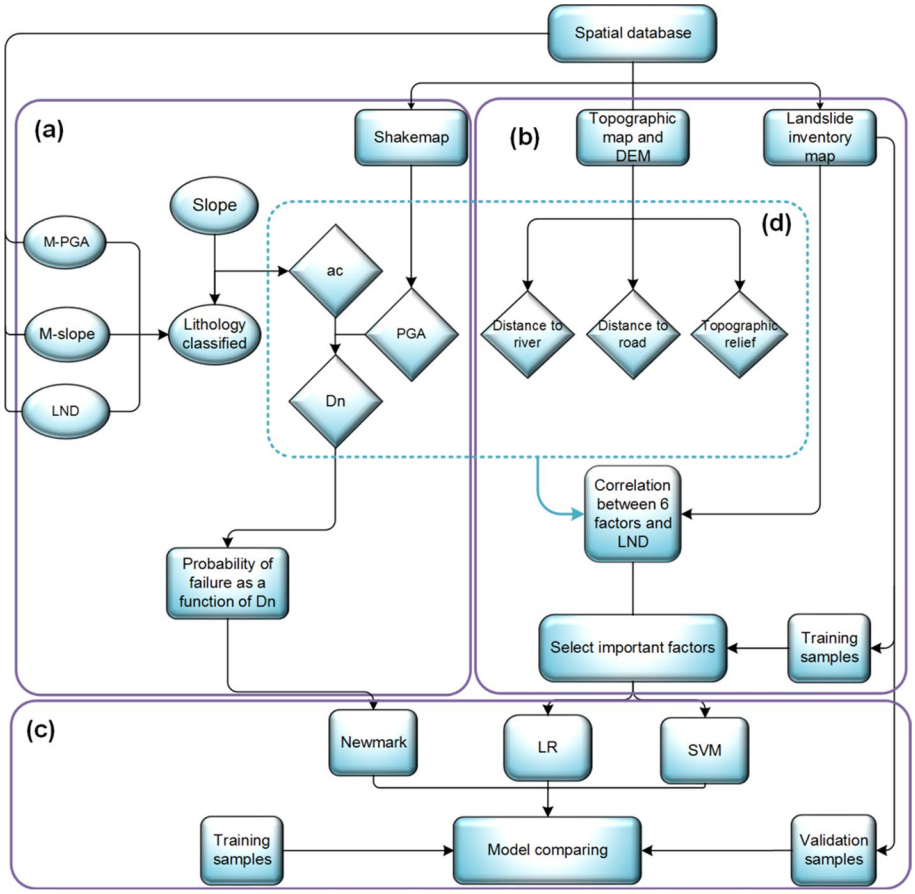

Fig. 7 Procedural flow chart of this study. **a** Technical route of simplified Newmark model; **b** technical route of statistical analysis models (LR and SVM); **c** landslide hazard mapping and model comparison; **d** six influencing factors used in analysis (a_c, PGA, D_n, topographic relief, distance to road, distance to river); M-PGA: average values of PGA in different lithology ages; M-slope: mean values of slope angle in various lithology ages; LND: landslide number density in various lithology ages

co-seismic landslides is mainly controlled by seismic, topographic and geological factors. Considering these conditions in the study area and other data, six influential factors were chosen. By analyzing the value of landslide number density (LND) in each classification of the factors, the influencing factors that have strong correlation with the landslide occurrence were selected as the evaluation parameters (independent variables) to establish the model.

4.1 Critical acceleration (a_c)

Previous research (Chen et al. 2014b) showed that critical acceleration (a_c) is a good and reliable criterion to assess slope stability. In fact, a greater a_c value means that a slope requires a greater force to overcome its stability. When the a_c value is low, sliding

occurs more easily on a slope. We divided critical acceleration (a_c) into groups according to the value of a_c, and the result (Fig. 8a) shows that there is a good negative correlation between critical acceleration (a_c) and the landslide number density (LND). LND decreases with the increase in critical acceleration (i.e., the greater the a_c is, the more stable the slope is, the less likely the slope is exposed to failure).

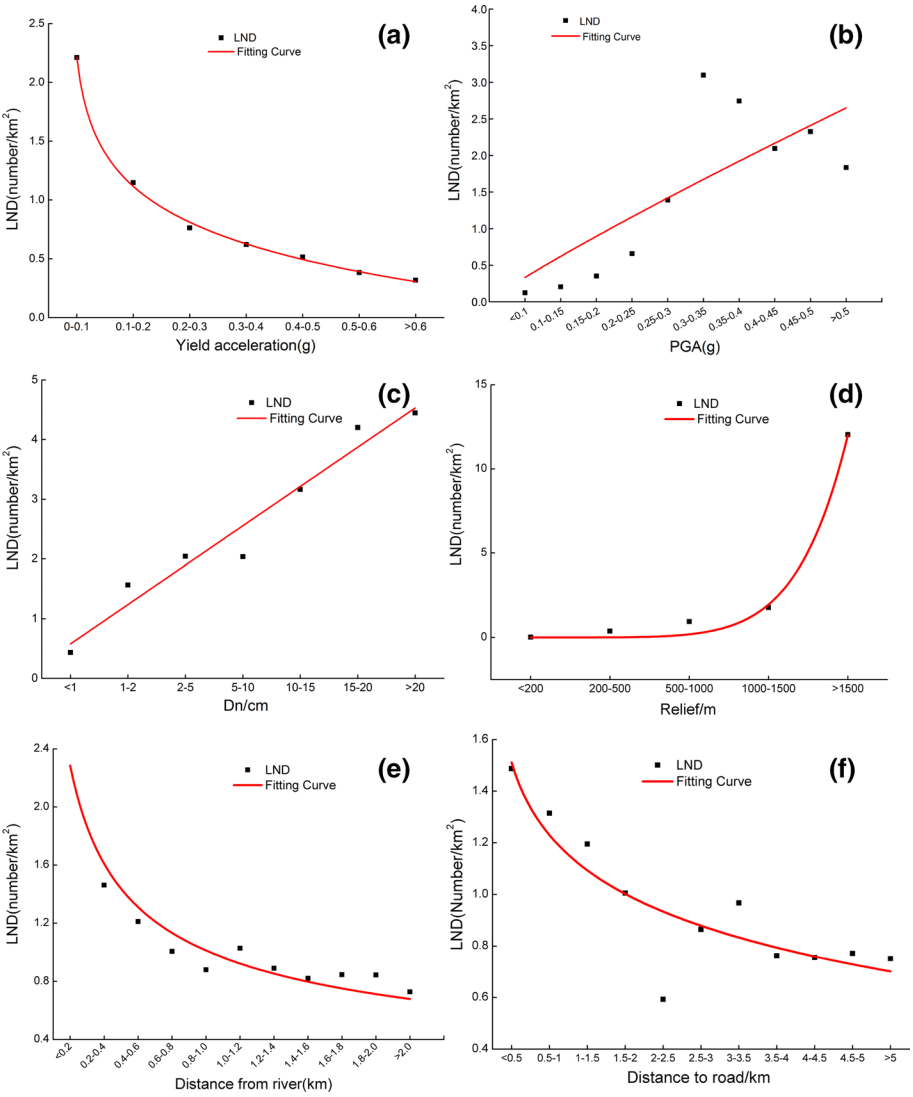

Fig. 8 Relationship between LND (landslide number density) and each related factor. **a** Yield acceleration (a_c), **b** PGA, **c** Newmark displacement (D_n), **d** topography relief, **e** distance to river, **f** distance to river

4.2 Peak ground acceleration (PGA)

PGA is one of the most important factors related to earthquake-triggered landslides, as in the cases of the 1999 Chi–Chi, the 2008 Wenchuan, and the 2013 Lushan earthquakes. It is often used as an important factor in landslide hazard assessment. Generally, The LND is positively correlated with the value of PGA, the higher the value of PGA is, the greater the possibility of landslide occurrence is. In this study, the PGA value was divided by 0.05 g into 10 groups. The result (Fig. 8b) shows that there is a poor positive correlation between the PGA value and the LND; the value of LND reaches the maximum in the range of 0.3–0.35 g, which is 3.1/km^2.

4.3 Newmark displacement (D_n)

We divided Newmark displacement (D_n) into groups and counted the value of LND in each group. The result (Fig. 8c) shows that on the whole, D_n has a good correlation with the LND (i.e., the greater the D_n value is, the greater the LND value is). But when the D_n is in the range of 5–10 cm, LND decreases with the increase in the D_n value. The main reason for this is probably that because the inputs into the Newmark analysis are poorly constrained, the outputs do not match observations very well.

4.4 Topographic relief

The study area is characterized by complex topography, with elevation decreasing from the west to the east. The maximum elevation is 5724 m, and the minimum is 336 m, 2851 m on average. The key of calculating the relief is to get the maximum and minimum elevation of the analysis window. Generally, the relief increases significantly with the growth of the analysis window. When the threshold is reached, the relief will not change significantly with the increase in the analysis window. This inflexion corresponds to the best analysis window. In this paper, based on the window increasing method, the inflexion was found by increasing the window gradually and calculating the terrain relief under different scales. Finally, the best analysis window was 2 km × 2 km (Jian et al. 2007). By processing the 10 m DEM, we obtained the topographic relief of the study area and counted the landslide density at different levels of the terrain relief (Fig. 8d). The result shows a positive correlation between the LND and the relief.

4.5 Distance to rivers

River banks can fail due to slope erosion. Many studies show that the proximity to the drainage lines is an important factor controlling the occurrence of landslides. In the study area, landslides occurred frequently on stream banks. To incorporate the effect of rivers on landslide initiation, we calculated the shortest distance from each landslide point to the rivers. Meanwhile, we constructed 11-class buffers from drainages with a 200 m interval and counted the value of LND in each class. The nonlinear negative logarithmic relationships between the distance to drainages and the landslide density at

Table 1 Multicollinearity diagnosis indexes for variables

Independent variables	Tolerance	VIF
Yield acceleration (a_c)	0.913	1.096
PGA	0.795	1.258
D_n	0.991	1.009
Topographic relief	0.792	1.262
Distance to rivers	0.512	1.954
Distance to roads	0.532	1.880

Table 2 Auto-correlation between these parameters

	a_c	D_n	PGA	Topographic relief	Distance to rivers	Distance to roads
a_c	1	−0.09	−0.03	0.22	0.09	0.16
D_n		1	0.03	0.03	−0.01	−0.01
PGA			1	−0.34	−0.33	−0.27
Topographic relief				1	0.21	0.03
Distance to rivers					1	0.67
Distance to roads						1

different levels are shown in Fig. 8e, indicating the LND decreases with the increase in the distance to drainage.

4.6 Distance to roads

The construction of mountain roads has a significant influence on the local physical geographical environment. Road construction may increase the instability of the slope. When driven by the collapsing force of an earthquake, both sides of roads are particularly prone to landslides. The shortest linear distance method was used to calculate the distance between each landslide site and the nearest road. The nonlinear relationships between the landslide density and different distances to roads from this work are shown in Fig. 8f. The LND decreases gradually with greater distance to roads, i.e., the closer the area to a road, the greater the density of landslides.

In logistic regression, multicollinearity diagnosis is necessary to check the correlation of independent variables. Tolerance (TOL) and the variance inflation factor (VIF) are two important indexes that are widely used for multicollinearity diagnosis. According to Hosmer and Lemeshow (2005), a TOL value less than 0.2 is an indicator for multicollinearity, and serious multicollinearity occurs between independent variables when the TOL values are smaller than 0.1. If VIF value exceeds 10, it is usually regarded as indicating multicollinearity. The TOL and VIF values in this study are shown in Table 1. It reveals that there is no multicolinearity between any of the factors.

The Pearson method is used to test the independence of the six factors. The correlation between the six factors w is shown in Table 2. The results show that the correlation coefficient between road distance and river distance is 0.67, and the linear correlation between other factors is weak.

Analyzing landslide density distribution between a_c and D_n, we found that due to the constrained input of PGA, LND does not increase with the increase in the D_n value in local areas. In addition, roads are often accompanied by rivers, resulting in a high linear correlation between the roads and rivers. So considering the above factors, we finally chose the 4 influencing factors, critical acceleration (a_c), topographic relief, PGA and distances to rivers as evaluation factors for building the evaluation model.

5 Results and analysis

In this study, LR was applied from the SPSS software and the coefficients were measured. Table 1 shows the extracted coefficients of the all variables by logistic regression analysis. The significance levels of the a_c values, PGA, distance to rivers, and topographic relief are all less than 0.05. The four variables are therefore considered to have a significant impact on the landslide occurrence. This statistical technique is a multivariate estimation that examines the relative strength and significance of factors. A positive sign indicates that the explanatory variable has increased the probability of change, and a negative sign implies the opposite effect. The result shows that PGA and topographic relief have positive correlations with landslide occurrences, with regression coefficients of 3.236 and 3.496, respectively; distance to rivers and a_c values have negative correlations with landslide occurrences, with regression coefficients of −2.828 and −2.224, respectively.

Equation (11) was derived according to the coefficients of logistic regression shown in Table 3, which was used to predict the possibility of landslide occurrence:

$$P = \frac{\exp\left(0.272 - 2.828\chi_1 + 3.236\chi_2 - 2.224\chi_3 + 3.496\chi_4\right)}{1 + \exp\left(0.272 - 2.828\chi_1 + 3.236\chi_2 - 2.224\chi_3 + 3.496\chi_4\right)} \tag{11}$$

where P is the estimated probability of landslide occurrence; χ_i represents the normalized values of causative factors.

The corresponding weight values were given to each causative factor according to the logistic regression coefficients, and the landslide hazard probability map of LR was prepared through the superposition operations of each causative factor layer (Fig. 9a).

The selection of the kernel function parameter and penalty parameter can affect the precision of the support vector machine significantly. The radial basis function (RBF) was used for the kernel, which is one of the most powerful kernel functions (Yao et al. 2008; Pradhan 2013). Previous research (Xu and Xu 2012; Xu et al. 2012b) showed the RBF kernel function may be more suitable for landslide susceptibility mapping. The mathematical

Table 3 Variables applied to the logistic regression equation

Variable	β	SE	Wals	Sig.[a]	Exp (β)
a_c (χ_1)	−2.828	0.219	167.010	0.000	0.059
PGA (χ_2)	3.236	0.141	526.288	0.000	25.429
Distance to rive (χ_3)	−2.224	0.236	89.077	0.000	0.108
Topographic relief (χ_4)	3.496	0.292	143.809	0.000	32.991
Constant	0.272	0.217	1.565	0.211	1.312

[a] All requested varibales entered

The significance levels of four independent variables are less than 0.05

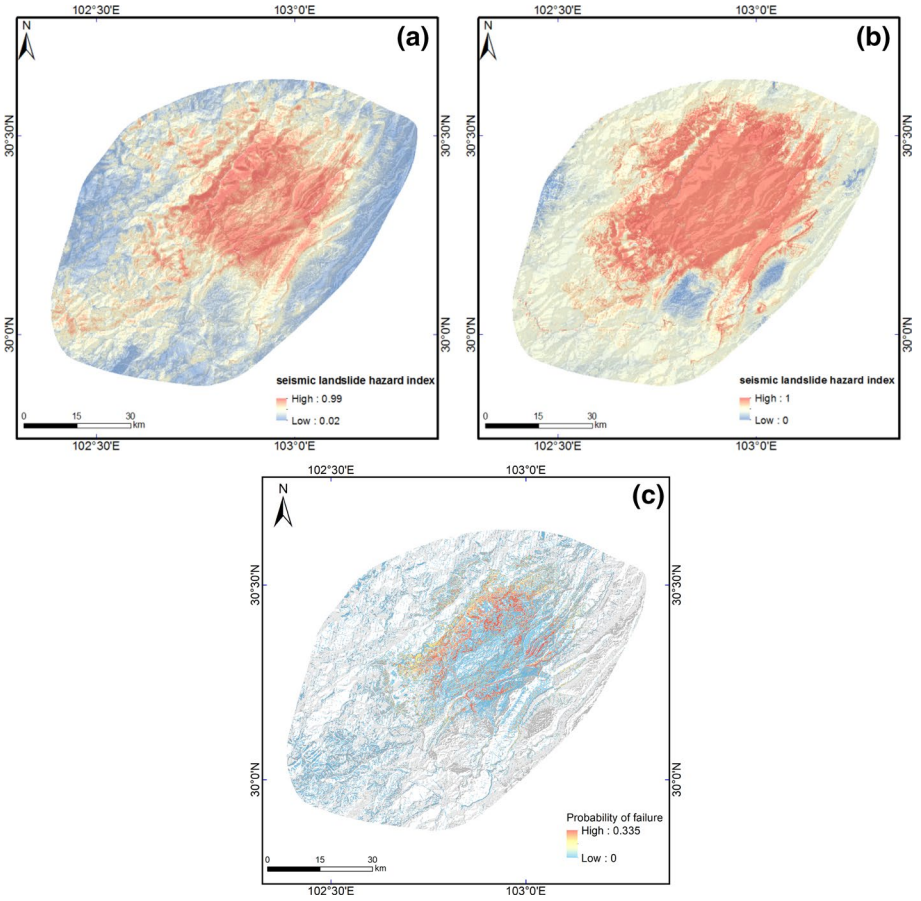

Fig. 9 Probability maps of Lushan earthquake triggered landslides using three methods. **a** LR, **b** SVM, **c** Newmark model

expression of the RBF function $K_{\mathrm{RBF}}(x - x')$ (Eq. 12) was employed in this study. In addition, the prediction capability of the SVM is also strongly influenced by the selection of the two parameters, C and g. Therefore, these parameters need to be carefully determined. C is the regularization parameter; if the value of C is large, it will lead to few training errors. In contrast, a small value of C will generate a larger margin and increase the number of training errors. The other parameter, g, manipulates the degree of nonlinearity in the SVM model. In this study, the best values of the two parameters were determined using the cross-validation algorithm based on MATLAB 2012b. Using the training dataset, the best C and g were determined as 64 and 5.65, respectively

$$K_{\mathrm{RBF}}(x - x') = \exp\left(-g||x - x'||^2\right). \tag{12}$$

Using the best pair of the RBF kernel parameters, the SVM model was constructed using the training data and then the model was applied to calculate landslide hazard index for the entire study area. Finally, landslide hazard probability map (Fig. 9b) in

the study area was created. The closer the value is to 0, the smaller the possibility of landslide occurrence is, and the closer the value is to 1, the greater the possibility of landslide occurrence is.

The D_n values represent the danger level of earthquake-induced landslides; the higher the D_n value is, the higher landslide occurrence is. Jibson et al. (2000) compared the locations of mapped landslides with the predicted displacement map and quantitatively evaluated the probability of failure (P_f) for different ranges of displacements with a Weibull curve (Eq. 13). In this study, we used this regression curve to prepare the landslide hazard probability map based on the D_n map of the 2013 Lushan earthquake. Finally, we prepared a probability map of slope failure based on the Newmark model (Fig. 9c), the probability of failure ranged from 0 to 0.335

$$P(f) = 0.335\left[1 - \exp\left(-0.048D_n^{1.565}\right)\right] \tag{13}$$

where D_n is the Newmark displacement in centimeters. Probability of failure ($p(f)$) is defined as the percentage of landslide cells within a displacement bin.

For LR and SVM, the landslide hazard index was ranked into four classes by interval 0.25, which are as follows: very low (0–0.25), low (0.25–0.5), moderate (0.5–0.75), and high (0.75–1). For Newmark model, the probability of failure was ranked into four classes by interval 0.1, which are as follows: very low (0–0.1), low (0.1–0.2), moderate (0.2–0.3), and high (0.3–0.4). Finally we obtained the hazard maps of Lushan earthquake-triggered landslides based on different models (Fig. 10). In order to compare the evaluation results of different methods, 15,546 landslides (area $\geq$ 100 m^2) triggered by the Lushan earthquake were counted. Figure 11 is the statistical results of the zoning area, the number of landslides and the landslide number density in different classes of different models.

The results show that in logistic regression, the area of high hazard class is 880.3 km^2, which accounts for 16.3% of the total study area. The number of landslides in this zone is 8977, accounting for 57.7% of the total landslides. 18.15% of the study area is designated as the middle hazard zone, where the number of landslides is 4278, accounting for 27.5% of the total number of landslides. On the whole, most landslides are concentrated in the middle and high hazard zones.

In SVM, the area of high hazard class is 1257.1 km^2, which accounts for 23.4% of the total study area. The actual number of landslides is 11,121, accounting for 71.5% of the total landslides. The area of middle hazard class is 2304.9 km^2, which accounts for 42.9% of the total study area. The number of landslides is 3585, accounting for 23.1% of the total number of landslides. Unlike the statistical results of the LR model, the area of very low hazard class based on SVM is smaller, only 12.8 km^2, which accounts for 0.2% of the study area. However, the area of very low hazard class based on LR model is 1260.1 km^2, which accounts for 23.4% of the study area.

In contrast, the evaluation results based on the Newmark model are relatively not good. Most landslides are concentrated in the very low hazard zone, where the number of landslides is 10,523, accounting for 67.6% of the total landslides. The area of high probability of failure class is 211.8 km^2, which accounts for 3.9% of the total study area, in which the number of landslides accounts for 16.1% of the total landslides.

Furthermore, we calculated the landslide number density in different hazard classes of the three models. From Fig. 11, we can see that the LND trend line of the Newmark model is very different from the LND trend lines of LR and SVM. The results of two statistical models (LR and SVM) show that the landslides density increases rapidly with the increase in the hazard level. For the Newmark model, massive landslides occurred in the area of

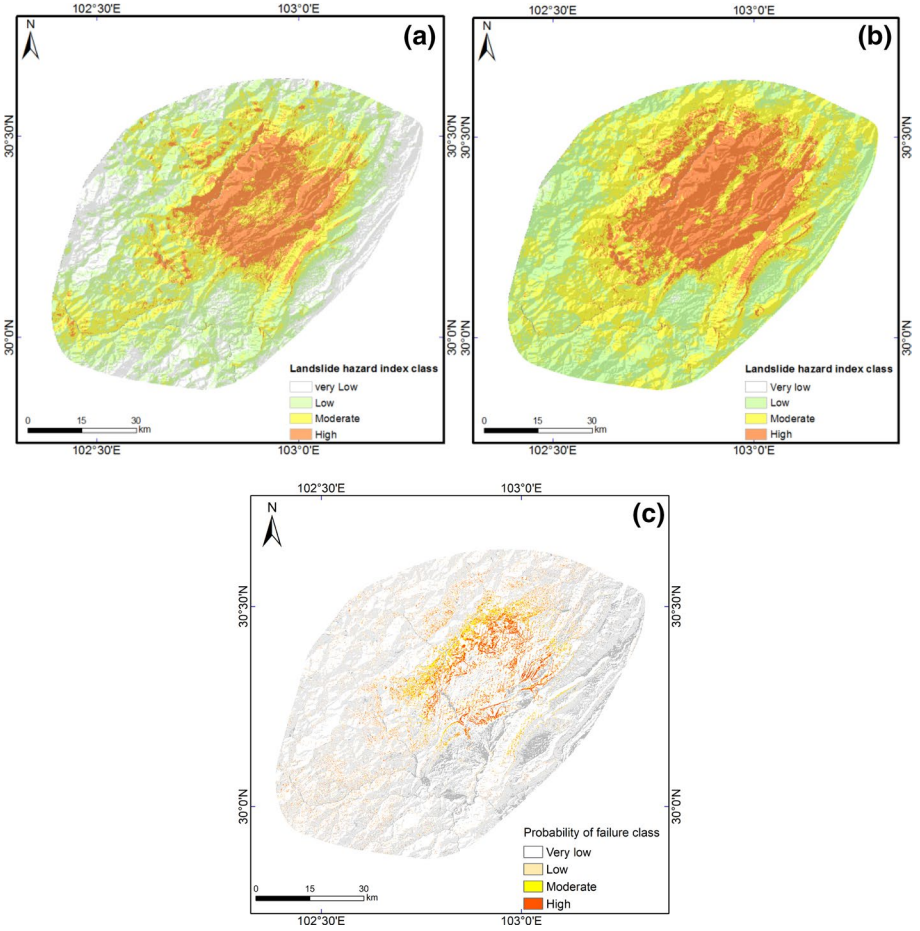

Fig. 10 Hazard maps of Lushan earthquake triggered landslides prepared by three methods. **a** LR, **b** SVM, **c** Newmark model

very low class, the landslide density in this area reaches 2.1/km^2, and landslide density does not increase with the increase in hazard level.

In this study, the ROC curve is also used to evaluate the accuracy of the models. In statistics, a receiver operating characteristic curve, i.e., ROC curve, is a graphical plot that illustrates the diagnostic ability of a binary classifier system as its discrimination threshold is varied. The ROC curve is a useful method of representing the quality of deterministic and probabilistic detection and forecast system (Swets 1988). The ROC curve plots the false positive rate (1-specificity) the *X* axis and 1-the false negative rate (sensitivity) on the *Y* axis. It shows the trade-off between the two rates. The area under the ROC curve (AUC) can be used for quantitative comparison of these models (Brenning 2005). If AUC < 0.5, the prediction result is opposite; AUC = 0.5, stochastic model; AUC between 0.5 and 0.7, the model has lower accuracy; AUC between 0.7 and 0.9, the model has higher accuracy; and AUC > 0.9 indicates an ideal model. The output results of the training set and the validation set were calculated, and the result of ROC curve was obtained (Fig. 12). The results

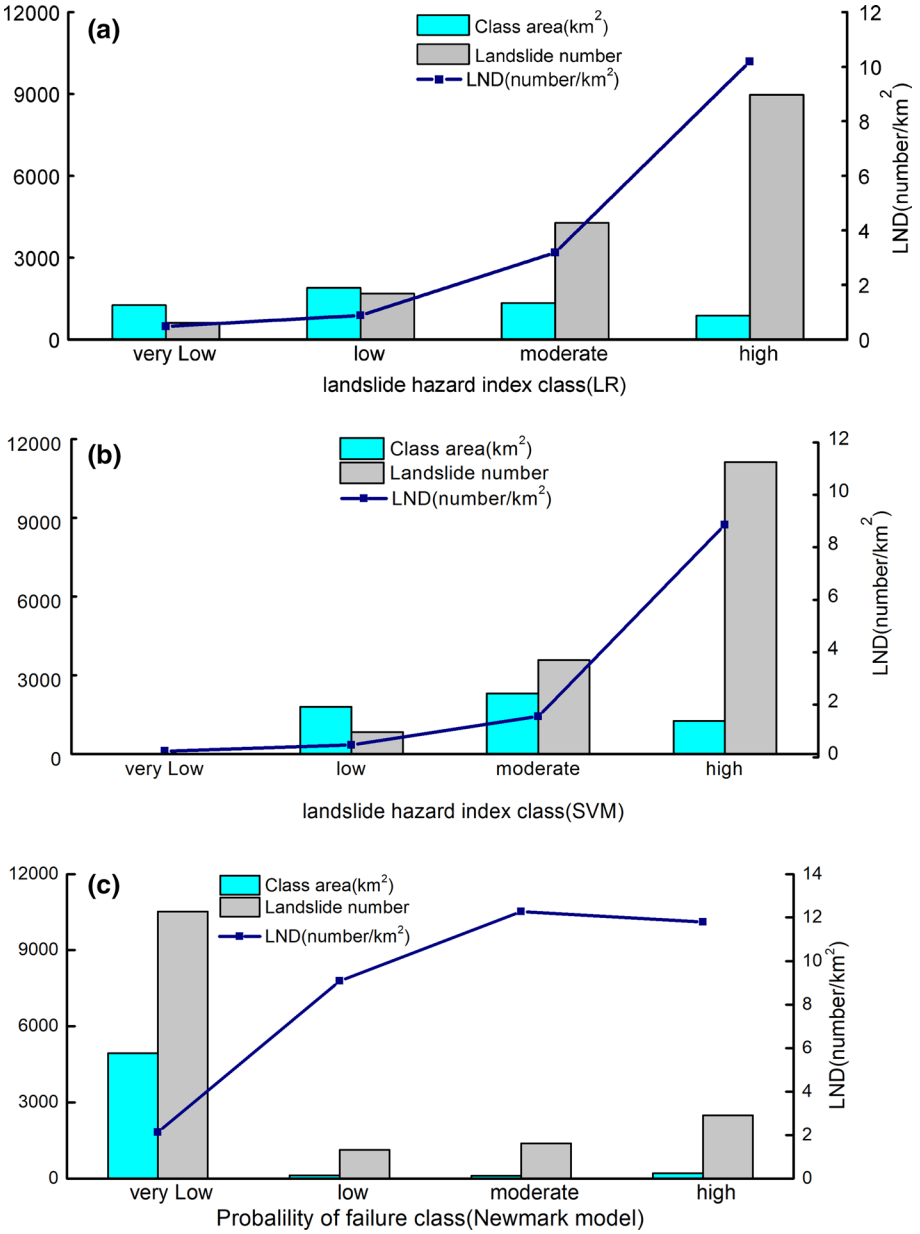

Fig. 11 Histogram showing relative distribution of various hazard levels and landslide occurrence from three methods. **a** LR, **b** SVM. **c** Newmark model

show that the two models of LR and SVM have good prediction accuracy, but the prediction results of Newmark model are not good. For training samples, the AUCs of LR and SVM are 0.810 and 0.823, respectively; the AUC of Newmark model is 0.736. For

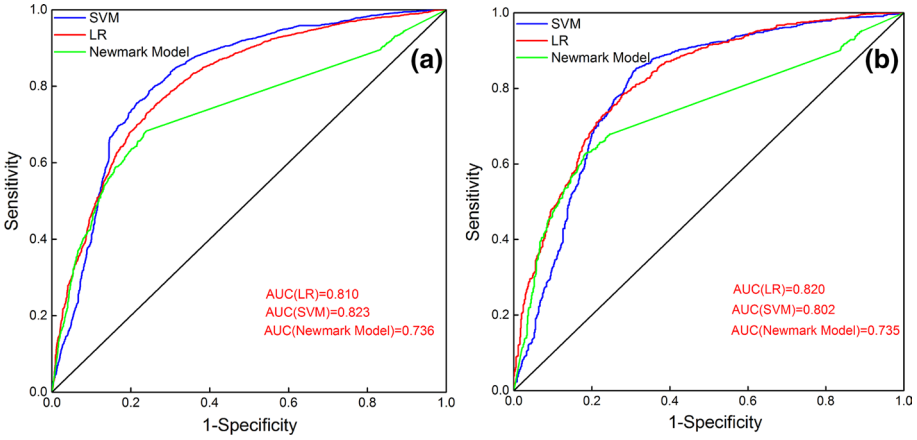

Fig. 12 ROC curves for LR, SVM and Newmark model. **a** Training samples set, **b** validating samples set

validating samples, the AUC is 0.820 for LR, 0.802 for SVM, and 0.735 for the Newmark model, respectively.

6 Discussion

Although a variety of methods (Akgun 2012; Althuwaynee et al. 2014; Hong et al. 2015; Kavzoglu et al. 2015) have been applied to landslide hazard evaluation, the accuracy of different evaluation models remains controversial. This work attempted to combine the Newmark model and the statistical analysis models (LR and SVM) to conduct the landslide hazard assessment of the Lushan earthquake, and to establish a more effective evaluation model. Based on the landslide density, average slope (mean slope) and average PGA (mean PGA) in various lithology ages, the lithology of the study area was more objectively grouped, and the critical acceleration (a_c) and the cumulative Newmark displacements (D_n) were mapped. We combined the statistical models and the output results of the Newmark model, while taking into account the induced mechanism of earthquake landslides and other controlling factors, to construct a new model. The result shows that the evaluation results based on this model have good prediction accuracy.

At present, Newmark analysis is widely used in assessment of co-seismic landslide hazard, while the practice shows its quantitative evaluation results have defects. The main reason is that in this method, it is difficult to reasonably estimate mechanical parameters of rock and soil and ground motion parameters. In this study, we grouped the lithology of the study area based on the inventory of Lushan earthquake landslides. But because of lacking the accurate PGA distribution in the study area, the values of D_n cannot permit to accurately predict the actual landslide distribution.

The earthquake ground motion is one of the most important factors in landslide hazard assessment, and PGA distribution map (issued by USGS) is the most common data source of it, so this study used a_c (intermediate output data of Newmark model), and PGA as influencing factors for the statistical methods. Meanwhile, we considered other influencing factors, such as river incision, topographic relief and artificial excavation, so that the

mechanism of earthquake landslides was taken into the statistical analysis method, and the limitation of the Newmark model was compensated.

From the distribution of landslide density, we can find that compared with the values of D_n, critical acceleration may reflect better the actual landslide distribution of the Lushan earthquake. In the Newmark model due to the constrained input data of PGA, the region where the value of critical acceleration (a_c) is less than the value of PGA is considered as landslide-free area, i.e., D_n value equal to 0. However, the actual distribution of Lushan earthquake landslides shows that a large number of landslides are present in the area with the D_n value equal to 0. This indicates that there is a big discrepancy between the actual landslide distribution and the prediction results based on the Newmark model by using poorly constrained strength and ground motion inputs, and the evaluation of the Newmark simple model is not good. In fact, according to accurate input parameters, the assessment results of the Newmark model may be close to the results based on statistical methods. However, in terms of current conditions, we cannot obtain the accurate input parameters which limit the output of the Newmark model.

From the evaluation results, this method combining the Newmark model and statistical method has a good prediction accuracy in landslide hazard assessment for the Lushan earthquake area. To some extent, this method overcomes the limitations of the Newmark model and greatly improves the accuracy of evaluation. But as we all know, based on the statistical analysis model, we need to use objective and complete landslide data to guarantee the accurate prediction result. The Newmark simplified model can carry out landslide hazard assessment without landslide samples. That is to say that the hazard assessment based on Newmark model can be achieved quickly after the earthquake, which cannot be achieved by statistical analysis model. So in the future, we will explore how to further combine these two evaluation methods for more accurate landslide hazard assessment by using a small amount of known landslides, providing an effective reference for the rapid assessment of the subsequent landslides in the earthquake-affected area.

7 Conclusions

The Newmark model and the statistical analysis models (LR and SVM) were combined to make a trial on landslide hazard assessment of the 2013 Lushan earthquake. The results show that critical acceleration may reflect better the actual landslide distribution in the Lushan earthquake-affected area compared with the accumulative displacement from the simplified Newmark model due to the constrained ground motion input. The statistical results of the zoning area, the number of landslides and the landslide number density of different models show that in logistic regression, the area of high hazard class accounts for 16.3% of the total study area, where the landslide number in is 8977; in SVM, 71.5% of the total landslides is in the area of high hazard class; in the Newmark model, more than 60% of the landslides are concentrated in the very low hazard area. This indicates that the prediction results based on the Newmark model are relatively not good. Furthermore, the ROC curves were used to evaluate the accuracy of the models. On the whole, the evaluation results of logistic regression model and support vector machine model have no difference. The results show that the two models of LR and SVM have good prediction accuracy. The AUC values of LR and SVM in training data set are 0.810 and 0.823, respectively; and those in validation data set are 0.820 and 0.802, respectively. While the prediction accuracy

of the Newmark model is relatively poor, with the AUC values for the training and validation data set 0.736 and 0.735, respectively.

Acknowledgements This study was supported by the National Natural Science Foundation of China (41472202).

References

Akgun A (2012) A comparison of landslide susceptibility maps produced by logistic regression, multi-criteria decision, and likelihood ratio methods: a case study at İzmir, Turkey. Landslides 9:93–106

Al-Homoud AS, Tahtamoni W (2000) Comparison between predictions using different simplified Newmarks' block-on-plane models and field values of earthquake induced displacements. Soil Dyn Earthq Eng 19:73–90

Althuwaynee OF, Pradhan B, Park HJ, Lee JH (2014) A novel ensemble bivariate statistical evidential belief function with knowledge-based analytical hierarchy process and multivariate statistical logistic regression for landslide susceptibility mapping. CATENA 114:21–36

Ayalew L, Yamagishi H (2005) The application of GIS-based logistic regression for landslide susceptibility mapping in the Kakuda-Yahiko Mountains, Central Japan. Geomorphology 65:15–31

Bai SB, Ping LU, Jian W (2015) Landslide susceptibility assessment of the Youfang Catchment using logistic regression. J Moutain Sci 12:816–827

Bray JD, Travasarou T (2007) Simplified procedure for estimating earthquake-induced deviatoric slope displacements. J Geotech Geoenviron Eng 133:381–392

Brenning A (2005) Spatial prediction models for landslide hazards: review, comparison and evaluation. Nat Hazards Earth Syst Sci 5:853–862

Chang CC, Lin CJ (2011) LIBSVM: a library for support vector machines. ACM Trans Intell Syst Technol 2:1–27

Chen XL, Yuan RM, Yu L (2014a) Applying the Newmark's model of the assessment of earthquake-triggered landslides during the Lushan earthquake. Seismol Geol 35:661–670 **(in Chinese)**

Chen XL, Liu CG, Yu L, Lin C (2014b) Critical acceleration as a criterion in seismic landslide susceptibility assessment. Geomorphology 217:15–22

Dai FC, Lee CF, Li J, Xu ZW (2001) Assessment of landslide susceptibility on the natural terrain of Lantau Island, Hong Kong. Environ Geol 40:381–391

Deng QD, Ran YK, Yang XP, Min W, Chu QZ (2007) Map of active fault in China. Seismological Press, Beijing **(in Chinese)**

Dreyfus DK (2011) A comparison of methodologies used to predict earthquake-induced landslides. PhD University of Texas

Dreyfus DK, Rathje EM, Jibson RW (2013) The influence of different simplified sliding-block models and input parameters on regional predictions of seismic landslides triggered by the Northridge earthquake. Eng Geol 163:41–54

Gallen SF, Clark MK, Godt JW (2015) Coseismic landslides reveal near-surface rock strength in a high-relief, tectonically active setting. Geology 43:11–14

Gallen SF, Clark MK, Godt JW, Roback K, Niemi NA (2016) Application and evaluation of a rapid response earthquake-triggered landslide model to the 25 April 2015 Mw 7.8 Gorkha earthquake, Nepal. Tectonophysics

Godt JW, Sener B, Verdin KL, Wald DJ, Earle PS, Harp EL, Jibson RW (2008). Rapid assessment of earthquake-induced landsliding. In: Tokyo, Japan: proceedings of the first world landslide forum

Guzzetti F, Carrara A, Cardinali M, Reichenbach P (1999) Landslide hazard evaluation: a review of current techniques and their application in a multi-scale study, Central Italy. Geomorphology 31:181–216

Hong H, Pradhan B, Xu C, Tien Bui D (2015) Spatial prediction of landslide hazard at the Yihuang area (China) using two-class kernel logistic regression, alternating decision tree and support vector machines. CATENA 133:266–281

Hosmer DW, Lemeshow S (2005) Multiple logistic regression, in applied logistic regression, 2nd edn. Wiley, New York, pp 31–46

Hu DY, Li J, Hao CY, Shui ZJ (2007) GIS-based landslide spatial prediction methods, a case study in Cameron Highland, Malaysia. J Remote Sens 11:852–859

Huang J, Zhou Q, Wang F (2015) Mapping the landslide susceptibility in Lantau Island, Hong Kong, by frequency ratio and logistic regression model. Geograph Inf Sci 21:191–208

Jian SC, Yong L, Kun YZ, Zhou N, Long ZL, Liang Y, Bo LJ (2007) Research on the DEM of topographic relief in Longmenshan river basin. J Sichuan Norm Univ 38:766–773
Jibson RW (1993) Predicting earthquake-induced landslide displacements using Newmark's sliding block analysis. Transportation Research Record
Jibson RW (2007) Regression models for estimating coseismic landslide displacement. Eng Geol 91:209–218
Jibson RW, Michael JA (2009) Maps showing seismic landslide hazards in Anchorage. Center for Integrated Data Analytics Wisconsin Science Center, Alaska
Jibson RW, Harp EL, Michael JA (1998) A method for producing digital probabilistic seismic landslide hazard maps: an example from the Los Angeles, California, area. Open-File Report
Jibson RW, Harp EL, Michael JA (2000) A method for producing digital probabilistic seismic landslide hazard maps: an example from the Los Angeles, California, area. Eng Geol 58:271–289
Kavzoglu T, Sahin EK, Colkesen I (2015) An assessment of multivariate and bivariate approaches in landslide susceptibility mapping: a case study of Duzkoy district. Nat Hazards 76:471–496
Kaynia AM, Skurtveit E, Saygili G (2011) Real-time mapping of earthquake-induced landslides. Bull Earthq Eng 9:955–973
Keefer DK (1984) Landslides caused by earthquakes. Geol Soc Am Bull 95:406
Lee S (2005) Application of logistic regression model and its validation for landslide susceptibility mapping using GIS and remote sensing data. Int J Remote Sens 26:1477–1491
Marjanović M, Kovačević M, Bajat B, Voženílek V (2011) Landslide susceptibility assessment using SVM machine learning algorithm. Eng Geol 123:225–234
McCrink TP (2001) Regional earthquake-induced landslide mapping using Newmark displacement criteria. San Cruz County, California, pp 77–92
Miles SB, Ho CL (1999) Rigorous landslide hazard zonation using Newmark's method and stochastic ground motion simulation. Soil Dyn Earthq Eng 18:305–323
Ministry of Construction of the People's Republic of China (2009) Code for geotechnical engineering investigation GB 50021-2001 (2009). National Bureau of Quality Inspection (**in Chinese**)
Ministry of Water Resources of the People's Republic of China (2014) Standard for engineering classification of rock masses GB/T 50218-2014. Standards Press of China, Beijing **(in Chinese)**
Newmark NM (1965) Effects of earthquakes on dams and embankments. Géotechnique 15:139–160
Nowicki Jessee MA, Hamburger MW, Allstadt K, Wald DJ, Robeson SM, Tanyas H, Hearne M, Thompson EM (2018) A global empirical model for near-real-time assessment of seismically induced landslides. J Geophys Res Earth Surf 123:1835–1859
Nowicki MA, Wald DJ, Hamburger MW, Hearne M, Thompson EM (2014) Development of a globally applicable model for near real-time prediction of seismically induced landslides. Eng Geol 173:54–65
Ohlmacher GC, Davis JC (2003) Using multiple logistic regression and GIS technology to predict landslide hazard in northeast Kansas, USA. Eng Geol 69:331–343
Pradhan B (2013) A comparative study on the predictive ability of the decision tree, support vector machine and neuro-fuzzy models in landslide susceptibility mapping using GIS. Comput Geosci 51:350–365
Pradel D, Smith PM, Stewart JP, Raad G (2005) Case history of landslide movement during the Northridge earthquake. J Geotech Geoenviron Eng 131:1360–1369
Rao G, Cheng YL, Lin AM, Yan B (2017) Relationship between landslides and active normal faulting in the epicentral area of the AD 1556 M ~ 8.5 Huaxian Earthquake, SE Weihe Graben (Central China). J Earth Sci 28:545–554
Rathje EM (2008) Probabilistic seismic hazard analysis for the sliding displacement of slopes. J Geotech Geoenviron Eng 134:804–814
San BT (2014) An evaluation of SVM using polygon-based random sampling in landslide susceptibility mapping: the Candir catchment area (western Antalya, Turkey). Int J Appl Earth Obs Geoinf 26:399–412
Saygili G, Rathje EM (2008) Empirical predictive models for earthquake-induced sliding displacements of slopes. J Geotech Geoenviron Eng 134:790–803
Swets JA (1988) Measuring the accuracy of diagnostic systems. Science 240:1285–1293
Umar Z, Pradhan B, Ahmad A, Jebur MN, Tehrany MS (2014) Earthquake induced landslide susceptibility mapping using an integrated ensemble frequency ratio and logistic regression models in West Sumatera Province, Indonesia. CATENA 118:124–135
Wilson RC, Keefer DK (1983) Dynamic analysis of a slope failure from the 6 August 1979 Coyote Lake, California, Earthquake. Bull Deismolog Soc Am 73:863–877
Xu C, Xu XW (2012) The 2010 Yushu earthquake triggered landslides spatial prediction models based on several kernel function types. Chin J Geophys 55:2994–3005 **(in Chinese)**

Xu XW, Wen XZ, Yu G, Chen G, Klinger Y, Hubbard J, Shaw J (2009) Coseismic reverse- and oblique-slip surface faulting generated by the 2008 Mw 7.9 Wenchuan earthquake, China. Geology 37:515–518
Xu C, Xu X, Dai F, Saraf AK (2012a) Comparison of different models for susceptibility mapping of earthquake triggered landslides related with the 2008 Wenchuan earthquake in China. Comput Geosci 46:317–329
Xu C, Dai F, Xu X, Yuan HL (2012b) GIS-based support vector machine modeling of earthquake-triggered landslide susceptibility in the Jianjiang River watershed, China. Geomorphology 145–146:70–80
Xu C, Xu XW, Yao Q, Wang Y (2013a) GIS-based bivariate statistical modelling for earthquake triggered landslides susceptibility mapping related to the 2008 Wenchuan earthquake, China. Q J Eng Geol Hydrogeol 46:221–236
Xu C, Xu XW, Dai FC, Wu Z, He H, Shi F, Wu X, Xu S (2013b) Application of an incomplete landslide inventory, logistic regression model and its validation for landslide susceptibility mapping related to the May 12, 2008 Wenchuan earthquake of China. Nat Hazards 68:883–900
Xu XW, Wen XZ, Han ZJ (2013c) Lushan Ms 7.0 earthquake: a blind reserve-fault earthquake. Chin Sci Bull 58:1887–1893
Xu C, Xu X, Yao X, Dai F (2014) Three (nearly) complete inventories of landslides triggered by the May 12, 2008 Wenchuan Mw 7.9 earthquake of China and their spatial distribution statistical analysis. Landslides 11:441–461
Xu C, Xu X, Shyu JBH (2015) Database and spatial distribution of landslides triggered by the Lushan, China Mw6.6 earthquake of 20 April 2013. Geomorphology 248:77–92
Xu C, Xu X, Tian Y, Shen L, Yao Q, Huang X, Ma J, Chen X, Ma S (2016) Two comparable earthquakes produced greatly different coseismic landslides: the 2015 Gorkha, Nepal and 2008 Wenchuan, China events. J Earth Sci 27:1008–1015
Xu C, Ma S, Tan Z, Xie C, Toda S, Huang X (2018) Landslides triggered by the 2016 Mj 7.3 Kumamoto, Japan, earthquake. Landslides 15:551–564
Yalcin A (2008) GIS-based landslide susceptibility mapping using analytical hierarchy process and bivariate statistics in Ardesen (Turkey): comparisons of results and confirmations. CATENA 72(1):1–12
Yao X, Tham LG, Dai FC (2008) Landslide susceptibility mapping based on support vector machine: a case study on natural slopes of Hong Kong, China. Geomorphology 101:572–582